

# Numerical simulations of two dimensional magnetic domain patterns

E. A. Jagla

*The Abdus Salam International Centre for Theoretical Physics  
Strada Costiera 11, (34014) Trieste, Italy*

(Dated: November 23, 2018)

I show that a model for the interaction of magnetic domains that includes a short range ferromagnetic and a long range dipolar anti-ferromagnetic interaction reproduces very well many characteristic features of two-dimensional magnetic domain patterns. In particular bubble and stripe phases are obtained, along with polygonal and labyrinthine morphologies. In addition, two puzzling phenomena, namely the so called ‘memory effect’ and the ‘topological melting’ observed experimentally are also qualitatively described. Very similar phenomenology is found in the case in which the model is changed to be represented by the Swift-Hohenberg equation driven by an external orienting field.

PACS numbers:

## I. INTRODUCTION

There is a surprisingly large number of systems that exhibit macroscopic textures arising from microscopic interactions.<sup>1</sup> To be concrete, I will take as a case of study that of patterns in magnetic systems (magnetic garnets<sup>2</sup> or ferrofluids<sup>3</sup>), but many of the conclusions obtained can be directly applied to other systems, as for instance, the mixed state of type I superconductors of slab geometry,<sup>4</sup> and Langmuir monolayers.<sup>5</sup> The phenomenology of these systems is qualitatively understood as appearing from the competition of two effects: a short range rigidity, and a long range (dipolar) interaction between the local magnetization at different spatial positions. Calculations suggest<sup>6</sup> that the ground state of the system consists of (i) a state of uniform magnetization, (ii) a hexagonal lattice of bubbles in a background with opposite magnetization, or (iii) a phase with alternating, parallel stripes of opposite magnetization. The parameter controlling which of these three is actually the ground state is the external magnetic field. However, in experiments, upon variation of the external field, different (typically metastable) flux configuration develop that originate in instabilities of the bubbles or the stripes. Most noticeable, these metastable configurations include labyrinthine phases of interpenetrating domains, and polygonal-like patterns.<sup>1</sup>

Model Hamiltonians that take into account the two relevant energy scales have been used to reproduce most of the elemental instabilities observed in experiments, in particular: the elongation and ‘fingering’ instability of bubbles,<sup>7</sup> and the undulation instability of stripes.<sup>8</sup> However, the much richer behavior of the full system, appearing from complex interaction effects in rather large spatial regions has not been studied in detail with this kind of models. In fact, it is not known if these simple models contain all necessary ingredients to produce realistic magnetization patterns over large spatial scales.

The main motivation of the present work is to present large scale simulations using a model Hamiltonian to see whether it can account for the full phenomenology and

the variety of morphologies observed. I claim that the answer is positive. The simulations are able to reproduce, in particular, two phenomena that have been observed in these systems and have remained largely as puzzles, namely, the so called ‘memory effect’<sup>9</sup> of some magnetic patterns, and the ‘topological melting’<sup>10</sup> of an ordered lattice of bubbles.

## II. DETAILS ON THE MODEL AND THE NUMERICAL TECHNIQUE

The model I will use is not at all new (see [1], [11] and references therein). I will consider a scalar field  $\phi(\mathbf{r})$  defined over the  $x$ - $y$  plane. This variable will represent the magnetization in the system, that in experiments is typically constrained (because of structural properties) to point perpendicularly to the  $x$ - $y$  plane. Then, experimentally, the magnetization  $\phi$  has a preference to take two different values, that without loss of generality I will assume to be  $\pm 1$ . It will be convenient for the simulations to consider  $\phi$  as a continuum variable and include in the Hamiltonian a local term  $H_l$  that favors the values  $\phi = \pm 1$ . This term will be of the form

$$H_l = \alpha_0 \int d\mathbf{r} \left( -\frac{\phi(\mathbf{r})^2}{2} + \frac{\phi(\mathbf{r})^4}{4} \right) - h_0 \int d\mathbf{r} \phi(\mathbf{r}) \quad (1)$$

and represents the simplest continuum field description of an Ising variable. Note that a term describing the effect of an external magnetic field  $h_0$  has been already included.

The other terms that will be included in the Hamiltonian are the following. First, there is a rigidity term  $H_{rig}$  of the form

$$H_{rig} = \beta_0 \int d\mathbf{r} \frac{|\nabla\phi(\mathbf{r})|^2}{2} \quad (2)$$

This term (with positive  $\beta_0$ ) discourages spatial variations of  $\phi$ , and can be called ‘attractive’, in the sense that two regions with a value of  $\phi$  of plus (or minus) one,

in a background of the opposite sign, tend to merge into a single one to reduce the value of this term (in fact, in a description in terms of an Ising variable on a lattice, this term maps onto a ferromagnetic interaction between nearest neighbor sites). The fact that our fundamental variable  $\phi$  is continuous rather than discrete, and the existence of the gradient term, imply in particular the existence of a natural width (of the order of  $\sqrt{\beta_0/\alpha_0}$ ) for the interface between domains with positive and negative magnetization. Choosing the parameters in such a way that this width is a few times the discretization distance in the simulation, allows to obtain a smooth interface between domains, which turns out to be very weakly pinned by the underlying numerical mesh, and whose energy is almost independent of its spatial orientation. These two facts are crucial for a realistic simulation, and cannot be easily achieved using a Ising variable that takes only two values (see for instances the attempts in [12]).<sup>13</sup>

Secondly, there is a term  $H_{dip}$  that models the dipolar interactions, of the form

$$H_{dip} = \gamma_0 \int d\mathbf{r} d\mathbf{r}' \phi(\mathbf{r}) \phi(\mathbf{r}') G(\mathbf{r}, \mathbf{r}') \quad (3)$$

where  $G(\mathbf{r}, \mathbf{r}') \sim 1/|\mathbf{r} - \mathbf{r}'|^3$  at long distances. At short distances however, the  $r^{-3}$  behavior has to be cut off to avoid divergences (in experiments, the cut off distance is given roughly by the thickness of the film). However, we can see that the way in which the cut off is done is not crucial for the results. In fact, we will take advantage of the fact that the two terms (2) and (3) can be compactly written in Fourier space as

$$H_{rig} + H_{dip} = \sum_{\mathbf{k}} |\phi(\mathbf{k})|^2 (\beta_0 k^2 + \gamma_0 G_{\mathbf{k}}) \quad (4)$$

where  $G_{\mathbf{k}}$  is the Fourier transform of  $G(\mathbf{r}, 0)$ . Thus, it is the combination  $(\beta_0 k^2 + \gamma_0 G_{\mathbf{k}})$  that will mostly determine the behavior of the system. Note that the short distance behavior of  $G$  in real space is masked in Fourier space at large  $k$  by the  $k^2$  term, and then is irrelevant. On the other hand, the  $r^{-3}$  behavior at long distances transforms into a  $k$  dependence of the form

$$G_{\mathbf{k} \rightarrow 0} = a_0 - a_1 |k|. \quad (5)$$

The constants can be exactly evaluated to be

$$a_0 = 2\pi \int_0^\infty r dr G(r) \quad (6)$$

$$a_1 = 2\pi \quad (7)$$

The finite value  $a_0$  of  $G_{\mathbf{k}}$  at  $k = 0$  reflects the fact that the interaction in real space is integrable (in spite of being sometimes called ‘long range’). Also note that  $a_1$  is independent of the short distance behavior of  $G(r)$ . The main features of the interaction in Fourier space are the maximum with finite derivative at  $k \rightarrow 0$ , and the minimum at a finite wave number  $k_{min} \sim \gamma_0/\beta_0$ . This

minimum exists for any non-zero  $\gamma_0$ , indicating that the effect of the dipolar interactions on large distances can never be neglected.

We have defined the energy function of the system, and now the dynamics has to be introduced. Since in magnetic systems the magnetization is a non-conserved order parameter, I will use the Allen-Cahn<sup>14</sup> dynamical equations, namely

$$\begin{aligned} \frac{\partial \phi(\mathbf{r})}{\partial t} &= -\lambda \frac{\delta(H_l + H_{rig} + H_{dip})}{\delta \phi(\mathbf{r})} = \\ &= -\lambda \left( \alpha_0 (-\phi + \phi^3) - h_0 - \beta_0 \Delta \phi + \gamma_0 \int d\mathbf{r}' \phi(\mathbf{r}') G(|\mathbf{r} - \mathbf{r}'|) \right) \end{aligned} \quad (8)$$

that represents an overdamped dynamics in which the system reduces its energy by a steepest descendant evolution. To efficiently implement these equations on the computer, and in order to avoid the direct evaluation of the integral in the last term of (8), a pseudo-spectral method<sup>15</sup> is used. I write the previous equation in Fourier space, namely

$$\frac{\partial \phi_{\mathbf{k}}}{\partial t} = -\lambda \left[ \alpha_0 (-\phi + \phi^3) \Big|_{\mathbf{k}} - h_0 \delta(\mathbf{k}) + (\beta_0 k^2 + \gamma_0 G_{\mathbf{k}}) \phi_{\mathbf{k}} \right] \quad (9)$$

In this way, the last term is now algebraic. The complication has been translated to the first term, that involves the evaluation of the Fourier transform of  $\phi^3$ . However, this can be done very efficiently by the use of standard fast-Fourier-transform techniques.

In the simulations below, the function  $G$  is defined in real space to be  $G(\mathbf{r}, \mathbf{r}') = 1/|\mathbf{r} - \mathbf{r}'|^3$  for any two points of the numerical mesh such that  $\mathbf{r} \neq \mathbf{r}'$ , whereas  $G(\mathbf{r}, \mathbf{r}) \equiv 0$ . Then the cut off distance is the lattice discretization. The Fourier transform of this expression on the square lattice gives for the relevant terms of  $G_{\mathbf{k}}$  the form of Eq. (5) with  $a_0 \simeq 9.05$ ,  $a_1 = 2\pi$ . Once the value of  $a_0$  is fixed (and since the value of  $a_1$  is universal), there are four independent coefficients in (9). Two of them can be fixed by rescaling the spatial and temporal coordinates. In fact, if we define a new field  $\tilde{\phi}(r, t) \equiv A^{-1} \phi(r/C, t/B)$  (and then  $\tilde{\phi}_{\mathbf{k}}(t) \equiv A^{-1} \phi_{\mathbf{k}}(t/B)$ ), and in case we choose  $A$  to be

$$A = \sqrt{1 + \frac{a_0 \gamma_0 (C - 1)}{\alpha_0}}, \quad (10)$$

the new field satisfies equations of motion that in Fourier space can be written as (the tilde in the new field has been eliminated for simplicity):

$$\frac{\partial \phi_{\mathbf{k}}}{\partial t} = \alpha (\phi - \phi^3) \Big|_{\mathbf{k}} + h \delta(\mathbf{k}) - (\beta k^2 + \gamma G_{\mathbf{k}}) \phi_{\mathbf{k}}, \quad (11)$$

with

$$\alpha \equiv \frac{\lambda \alpha_0 A^2}{B} \quad (12)$$

$$h \equiv \frac{\lambda h_0}{AB} \quad (13)$$

$$\beta \equiv \frac{\lambda \beta_0 C^2}{B} \quad (14)$$

$$\gamma \equiv \frac{\lambda \gamma_0 C}{B} \quad (15)$$

and where  $G_{\mathbf{k}}$  is (up to the linear terms that are relevant for our analysis) the same function as before, namely  $G_{\mathbf{k}} = a_0 - a_1|k|$  with the same  $a_0$  and  $a_1$ . This renormalization can be used to fix two parameters in the new non-dimensional equations (11). In the simulation presented below I have fixed  $\beta = 2.0$ ,  $\gamma = 0.19$  and took the spatial discretization to be the unit of length (this choice was convenient when implementing the equations on the numerical mesh, and have no other particular meaning). Therefore, we see that in addition to the external control parameter  $h$ , a single internal control parameter  $\alpha$  remains. This parameter regulates the possibility of the field  $\phi$  to take values others than the most convenient ones, namely  $\phi = \pm 1$ . We will see below the different morphologies that appear for different values of  $\alpha$ . From now on I will always refer to the non-dimensional form (11) of the equations of motion.

Starting from an arbitrary initial condition, Eq. (11) describes an evolution in which the total energy of the system  $H_l + H_{rig} + H_{dip}$  is steadily reduced until it reaches a minimum, in which  $\partial \phi_{\mathbf{k}} / \partial t$  is identically zero. We will see that typically the true minimum of the system is not reached, but instead one of many possible metastable states is obtained. The simulations presented below were done on a  $512 \times 512$  mesh using periodic boundary conditions. The time-integration of the equations is done using a semi-implicit first order method, in which the  $k^2$  term in Eq. (11) is evaluated in the new time value. Concretely, I use an iteration scheme based on the following discretized form of (11)

$$\frac{\phi_{\mathbf{k}}^{t+\delta t} - \phi_{\mathbf{k}}^t}{\delta t} = \alpha(\phi - \phi^3)|_{\mathbf{k}}^t + h\delta(\mathbf{k}) - \gamma G_{\mathbf{k}}\phi_{\mathbf{k}}^t - \beta k^2 \phi_{\mathbf{k}}^{t+\delta t}. \quad (16)$$

This treatment of the diffusive term is standard to improve the stability of the algorithm.<sup>16</sup> In all cases below the time interval used is  $\delta t = 0.5$ .

### III. RESULTS

The initial condition for the variable  $\phi$  is taken to be locally random in the interval  $-1 < \phi < 1$ , and the system is evolved during an equilibration time  $t_{start}$  in the presence of a fixed applied external field  $h_{start}$ . If  $h_{start}$  is too large, the configuration obtained turns out to be a state of uniform magnetization. However, for lower  $h_{start}$ , a structure of bubbles of the minority phase (with magnetization anti-parallel to the field) within a background of the opposite magnetization may be favored.

After the time  $t_{start}$ , the field is decreased as a function of time with a finite rate  $dh/dt$ . This value is taken

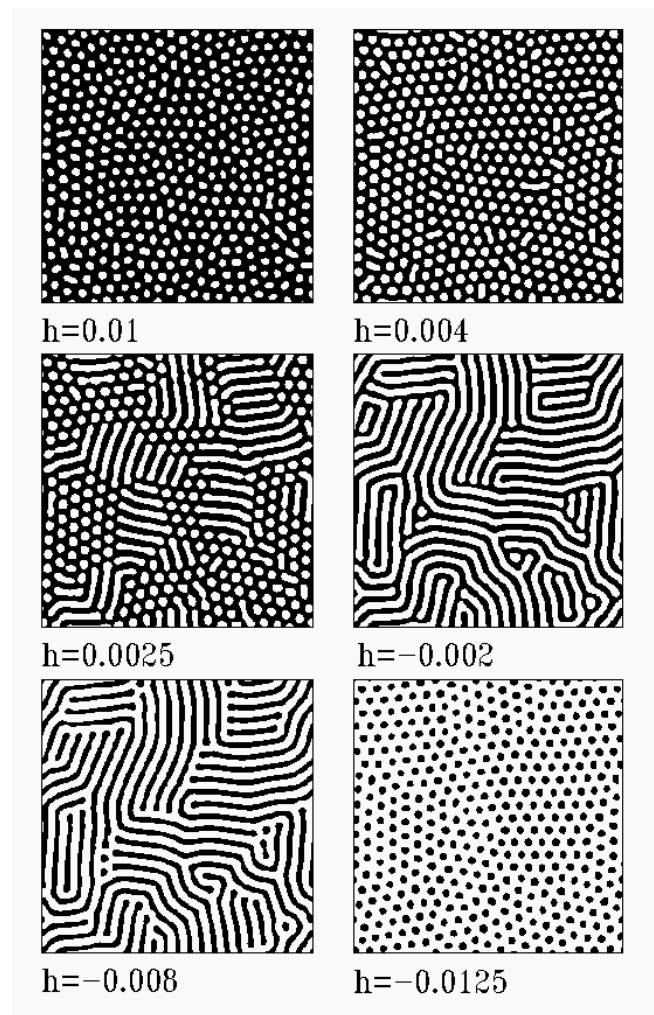


FIG. 1: Evolution of the magnetization distribution upon reduction of the magnetic field  $h$ , for  $\alpha = 1.6$ . Other parameters are:  $t_{start} = 3000$ ,  $h_{start} = 0.01$ ,  $dh/dt = -5 \times 10^{-7}$  (see text). Here and in the following figures black (white) indicates regions with positive (negative) magnetization, all parameters are in the non-dimensional form corresponding to Eq. (11), and system size is  $512 \times 512$ .

to be as small as possible (within reasonable computing time) in order that the field change can be considered to be adiabatic (we will see that this cannot always be guaranteed due to the existence in some cases of field driven instabilities). During the evolution, different morphologies are observed for different values of  $\alpha$  in Eq. (11), which will be described now.

*Almost reversible interconversion of bubbles and stripes.* For  $\alpha = 1.6$ , the result obtained is shown in Fig. 1. Starting from the initial bubble phase, upon reduction of the field  $h$ , neighbor bubbles coalesce, forming a striped pattern. When the field becomes negative, the stripes destabilize, and separate in a chain of bubbles, which have opposite magnetization with respect to the original ones. The sequence of bubble and stripe patterns is found to be reversible upon cycling of the field.

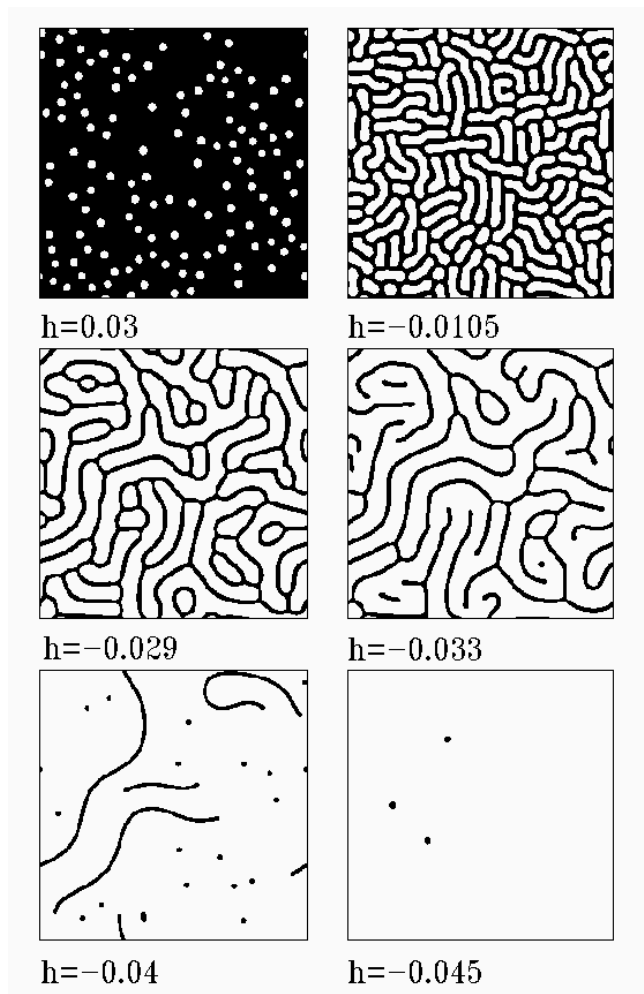


FIG. 2: Same as Fig. 1 for  $\alpha = 1.8$  ( $t_{start} = 1500$ ,  $h_{start} = 0.03$ ,  $dh/dt = -3 \times 10^{-6}$ ).

There is however a noticeable hysteresis in the field value at which the bubble-stripe interconversion occurs. This is just the consequence of the transition between bubbles and stripes being first order.<sup>6</sup>

*From bubbles to rather isolated and wandering stripes.* For a slightly larger value of  $\alpha$ , namely  $\alpha = 1.8$  (Fig. 2), the bubbles may become unstable and elongate individually, without merging with their neighbors at the beginning. When they finally merge (for  $h \lesssim -0.025$ ), regions with positive magnetization generate wavy stripes of well defined thickness. Contrary to the previous case, these regions do not separate into ‘beads’ when the field is made more negative, but eventually retract back to a single spot of positive magnetization that eventually disappears.

*Collapse of the bubbles to a polygonal pattern.* For larger values of  $\alpha$ , the bubbles are seen to remain (meta-) stable down to a field where they start to merge with their neighbors, but now in a sort of two dimensional way, as seen in Fig. 3 for  $\alpha = 2.2$ . This has to be compared with the previous case where the initial collapse of bubbles was

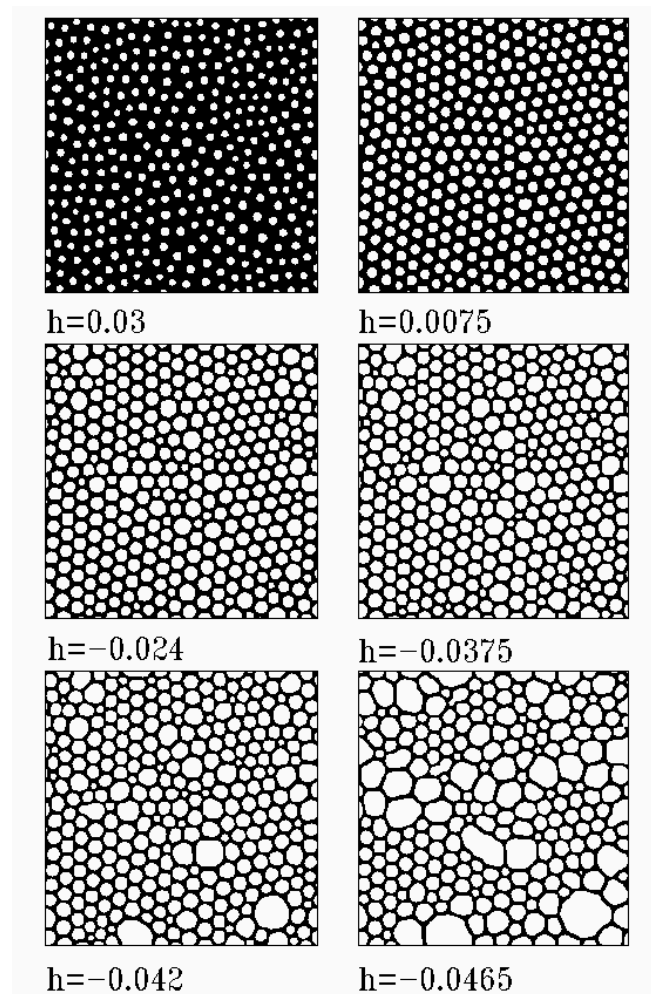


FIG. 3: Same as Fig. 1 for  $\alpha = 2.2$  ( $t_{start} = 4500$ ,  $h_{start} = 0.03$ ,  $dh/dt = -1 \times 10^{-6}$ ).

mainly one-dimensional, generating stripes (see the cases  $h = -0.029$  and  $h = -0.033$  in Fig. 2). In the present case, the collapse of neighbor bubbles seems to occur as a cascade process, where some initial coalescences trigger the full transition of the lattice. In fact, in Fig. 4 the field was kept constant at the value  $h = -0.0465$  (corresponding to the last panel in Fig. 3), and the evolution was followed as a function of time. A coarsening process is occurring here. Actually, the last pattern in Fig. 4 is not totally relaxed yet. Incidentally note in the last panel of Fig. 4 the existence of small pentagonal bubbles, highlighted by the arrows. This structure has been observed experimentally to be ubiquitous, and very stable.<sup>10</sup>

This case suggests the following interesting result: if a perfect original pattern of bubbles is constructed by hand, it can remain stable for values of the field at which the disordered bubble system would have already collapsed. Now, if in this ordered, metastable structure, a defect is introduced, it can completely disorder the lattice. In fact, we see in Fig. 5 how the presence of the defect produces a sequence of instabilities that destroy

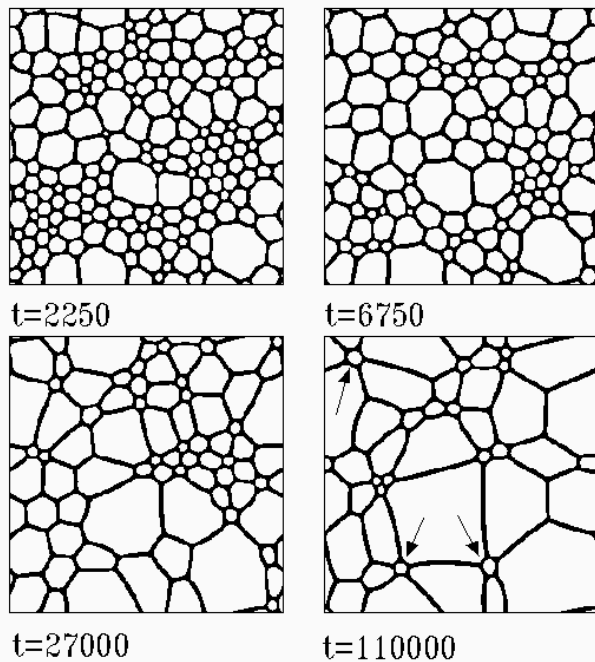


FIG. 4: The final configuration if Fig. 3 evolved at constant field  $h = -0.0465$  as a function of time, as indicated ( $t = 0$  corresponds to the last panel in Fig. 3). Arrows in the last panel highlight some small pentagonal bubbles, a structure that appears ubiquitous both in experiments and in the simulations.

many of the walls between neighbor bubbles, generating a rather well defined disordering front that leaves behind a disordered structure with much lower magnetization. This effect has been experimentally observed and called *topological melting*<sup>10</sup> of the bubble lattice. It has been observed to occur (although in a less dramatic form) also for systems in which the long range interaction is of Coulomb type<sup>17</sup>.

*Labyrinthine patterns and the memory effect.* If from the last panels in Figs. 2 or 4 the field is slowly switched off, interesting results are obtained. In the case in which we start from the configuration of the last panel in Fig. 2, which contains three (meta-) stable spots of positive magnetization, they remain stable (increasing only slightly in size) up to  $h \sim -0.02$ . At this field an instability occurs, the bubbles becoming unstable. If we maintain the field fixed at a value slightly lower (in absolute value) than the instability value, we obtain the results presented in Fig. 6, which shows snapshots as a function of time, for a fixed value of the field  $h = -0.018$ . The bubbles elongate and successively branch, forming labyrinthine patterns that invade the whole sample. On the other hand, if the field that we apply is much beyond the instability value (Fig. 7) the evolution is more rapid, and with a larger degree of branching of the magnetic domains. Note the difference in the degree of branching in the final patterns of Figs. 6 and 7. The greater tendency to branching when

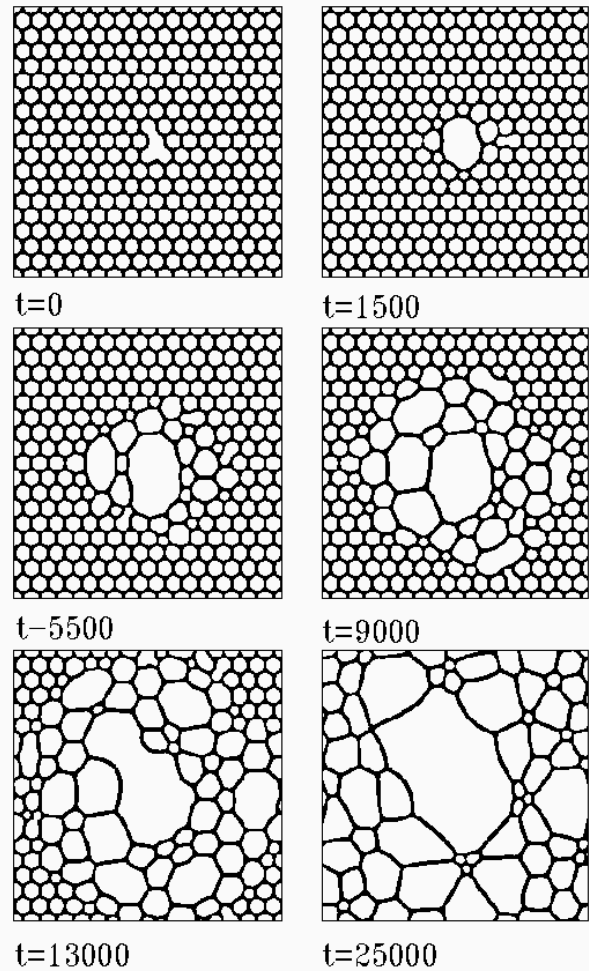


FIG. 5: Topological melting of an order array of bubbles for  $\alpha = 2.2$ , upon the *ad hoc* inclusion of a defect in the middle of the sample. The evolution occurs at a fixed value of the field  $h = -0.05$ , as a function of the simulation time, as indicated.

the applied field is more and more beyond the instability value is well known experimentally and theoretically<sup>7</sup>. This kind of instability is also similar to that observed in some reaction-diffusion systems<sup>18</sup>.

If we reduce the absolute value of the field from a configuration in which stripes are already present, we observe an undulation transition<sup>8</sup> at a field with larger absolute value than before. But contrary to what happened in Figs 6 and 7, if the field is changed slowly the system evolves smoothly (no instability appears), and stripes do not branch. Positive magnetization regions invade the system through wandering of the stripes, but new branches do not appear or are very rare.

In particular, in the case in which we reduce the field starting from the last configuration in Fig. 4 in which stripes are abundant as walls between polygons, the undulation occurs mildly, with almost no breaking or reconnection of the cell walls, and then the final labyrinthine pattern at  $h = 0$  is topologically equivalent to the orig-

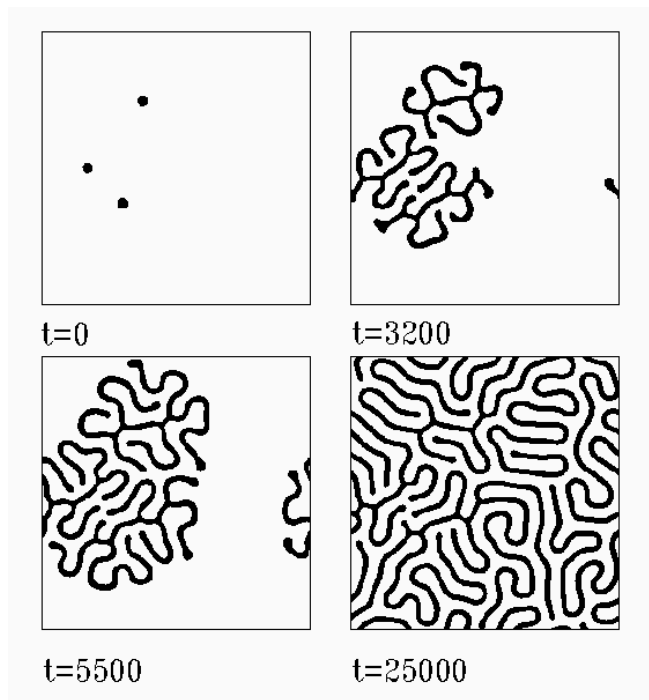


FIG. 6: Time evolution of the pattern shown in the first panel upon the application of a constant field ( $h = -0.018$ ) slightly beyond the critical field at which those bubbles destabilize. Times of the snapshots are indicated.

inal one. This is shown in Fig. 8. A nice consequence of this, is that when the field is switched on again (last panels in Fig. 8), the original pattern is almost recovered. This effect, called the *memory effect*<sup>9</sup> has been observed experimentally, and the typical evolution of the patterns over many cycles of the field has been analyzed. We are seen that this effect is contained in the simple model Hamiltonian we are using.

#### IV. DISCUSSION AND CONCLUSIONS

Summarizing, in the previous Section I have shown how the model equations (11) can be efficiently simulated in systems of reasonably large size. In this way, we have seen emerging most of the phenomenology of two dimensional magnetic patterns and other similar systems. The success of the present numerical simulations are due to a combination of reasons, mainly: the use of a continuum variable instead of a discrete one to obtain smooth domain walls between regions with opposite values of  $\phi$ , and the use of pseudo-spectral techniques to evaluate efficiently the ‘long-range’ dipolar force. These facts combine to allow a realistic simulation of domain patterns that show many of the features observed in experimental realizations. In particular, the *memory effect*<sup>9</sup> and the *topological melting*<sup>10</sup> of the system are very well reproduced.

I want to emphasize that in all cases I have studied, the

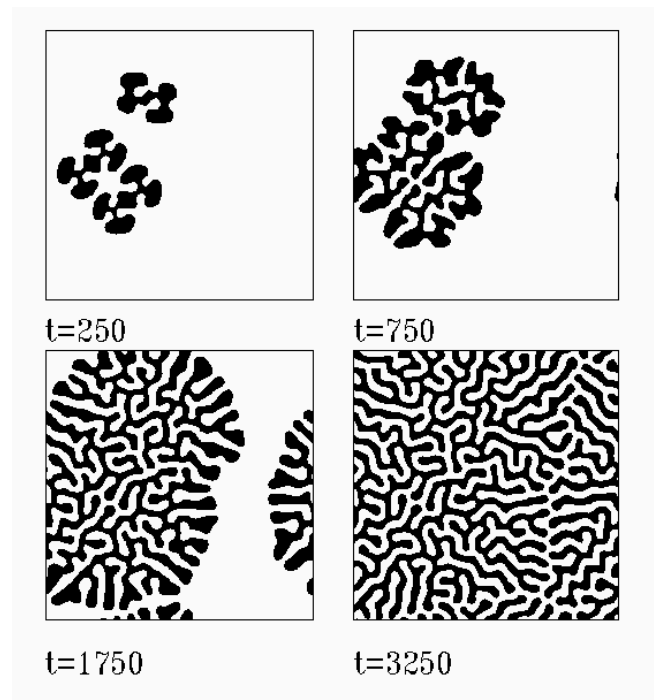


FIG. 7: Same as Fig. 6 for  $h = 0$ , i.e., here the system is brought deeply inside the instability region. Note the much larger amount of stripe branching in the final (stable) pattern, and the shorter time scale as compared with the previous figure.

evaluation of the total energy of the system is compatible with the fact that the only patterns truly corresponding to the ground state of the system are: (i) a pattern with uniform magnetization if the field is strong enough, (ii) a regular bubble phase for intermediate fields, and (iii) a regular stripe phase for low (including zero) field. Although this is not a demonstration that they are the only possible ground states, it points in this direction, and it is in agreement with the results of theoretical studies.<sup>6</sup> The other patterns observed (labyrinthine, polygonal, etc.) are seen to be metastable, and they are originated in the particular cycling of the field (and in the initial conditions) to which the sample is subjected. A recent experimental study<sup>19</sup> has shown in fact how the labyrinthine patterns converge to parallel stripes upon relaxation.

Very different morphologies have been observed when the parameter  $\alpha$  in Eq. (11) is changed. Figs. 3, 4, and 8 (corresponding to the largest values of  $\alpha$ ) compare very well with the patterns observed in magnetic garnets and ferrofluids (see [1], [10], and [11]). The results for lower  $\alpha$  (in particular, Figs. 1 and 2) are more akin to Langmuir monolayers<sup>5</sup> and flux structures in type I superconductors.<sup>4</sup> This suggests that in real systems the possibility of the order parameter to take values different than the two preferred ones can influence noticeable the physical properties.

I want to mention here that the present model can be also efficiently used to study the effect of quenched disor-

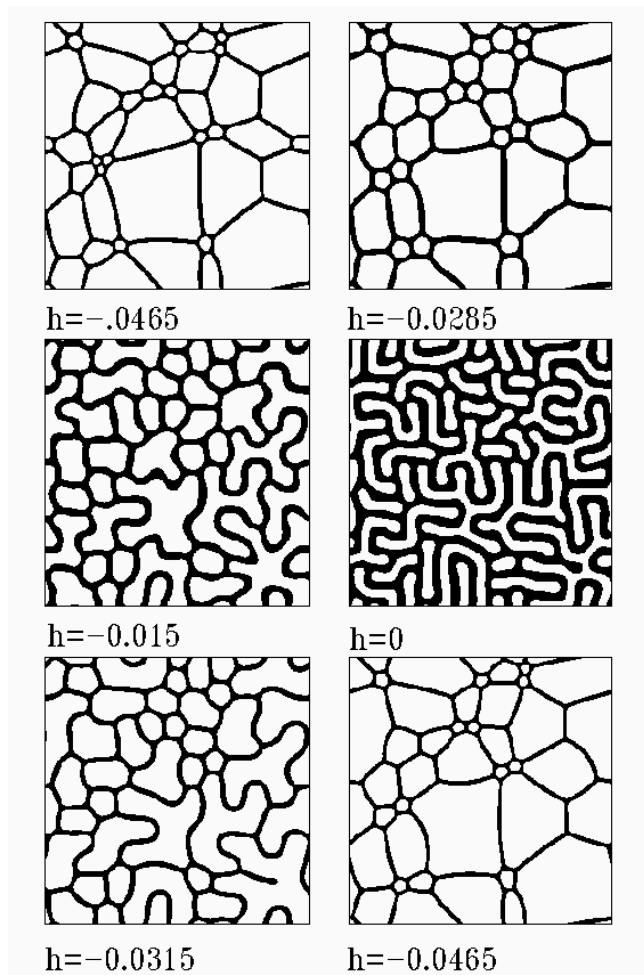


FIG. 8: Reducing the field from the final configuration in Fig. 4 down to  $h = 0$  and back to its original value ( $|dh/dt| = 1 \times 10^{-6}$ ). Note the ‘memory’ of the pattern as comparing first and last panels.

der in the system, and the effect of thermal fluctuations. Preliminary results indicate that the model generates hysteresis curves and magnetization patterns that, as a function of the amount of disorder, compare very well with experimental ones<sup>20</sup>. These results will be published separately.

We have seen that in the present model the dynamics is controlled by an interaction function in  $k$  space that has a maximum with finite derivative at  $k \rightarrow 0$  and a minimum at a finite  $k_{min}$  value. It is worth comparing this

case with respect to other possibilities. One is the case in which the field  $\phi$  is considered to be charged, instead of carrying a dipole. Two cases can be considered. One is that of true three dimensional charges ( $G(r) \sim r^{-1}$ ) and the other is the case of two dimensional charges ( $G(r) \sim -\ln(r)$ ). In both cases, the interaction in  $k$  space gets a divergence at low  $k$ . This model has been studied in detail in [17] (see the references in there for realizations of this case). There, instabilities of a single bubble have been found which are similar to those I find in the dipolar system. It remains to be seen if the other effects described here are also present in Coulombic systems.

Another case to compare with is that of interactions decaying in real space more rapidly than  $r^{-3}$ . In this case, a  $k$  space interaction with a quadratic maximum at  $k = 0$  is obtained. If this maximum dominates over the quadratic minimum coming from the  $\Delta\phi$  term in Eq. (8), then the effective interaction has a quadratic maximum at the origin and a minimum at some finite  $k_{min}$ . This case corresponds qualitatively to the interaction considered in the Swift-Hohenberg equation.<sup>21</sup> For this interaction, and controlling the same parameter  $\alpha$  as I did here, I have obtained basically all the effects and morphologies described in the previous section. On one hand this tells that the singularity at  $k = 0$  of the dipolar interaction is not crucial in obtaining these effects, a quadratic maximum suffices. On the other hand it is a bit surprising that in the wide literature related to the Swift-Hohenberg equation these effects have not been described previously. This might be due to the fact that the Swift-Hohenberg equation is usually considered in the absence of a ‘magnetic-field-like’ term that favors one of the two orientations, and this term is crucial to obtain the metastable patterns. It is then likely that the much studied relaxation to equilibrium properties of the patterns seen in the Swift-Hohenberg equation and the coarsening properties of the magnetic patterns (studied for instance in [9]) can be put under the same framework. I hope the present work encourages some studies in this direction.

## V. ACKNOWLEDGMENTS

I thank J. R. Iglesias for useful comments on an early version of the manuscript.

<sup>1</sup> M. Seul and D. Andelman, *Science* **267**, 476 (1995); F. Elias, C. Flament, J.-C. Bacri, and S. Neveu, *J. Phys. I France* **7**, 711 (1997).

<sup>2</sup> M. Seul, L. R. Monar, L. O’Gorman, and R. Wolfe, *Science* **254**, 1616 (1991); M. Seul and R. Wolfe, *Phys. Rev. A* **46**, 7519 (1992); *ibid.* **46**, 7534 (1992).

<sup>3</sup> R. E. Rosensweig, *Sci. Am.* **247**, 124 (October 1982).

<sup>4</sup> R. Huebener, *Magnetic Structures in Superconductors*, Springer-Verlag, Berlin (1979); A. T. Dorsey and R. E. Goldstein, *Phys. Rev. B* **57**, 3058 (1998); H. Bokil and O. Narayan, *Phys. Rev. B* **56**, 11195 (1997).

<sup>5</sup> D. J. Keller, H. M. McConel, and V. T. Moy, *J. Phys.*

- Chem. **90**, 2311 (1986); D. Andelman, F. Brochard and J.-F. Joanny, J. Chem. Phys. **86** 3673 (1987); M. Seul and M. J. Sammon, Phys. Rev. Lett. **64**, 1903 (1990); K. J. Stine, S. A. Raueo, B. G. Moore, J. A. Wise, and C. M. Knobler, Phys. Rev. A **41**, 6884 (1990); M. Seul and V. S. Chen, Phys. Rev. Lett. **70**, 1658 (1993).
- <sup>6</sup> T. Garel and S. Doniach, Phys. Rev. B **26**, 325 (1982); K.-O. Ng and D. Vanderbilt, Phys. Rev. B **52**, 2177 (1995); R. de Koker, W. Jiang, and H. M. McConnell, J. Phys. Chem. **99**, 6251 (1995).
- <sup>7</sup> S. A. Langer, R. E. Goldstein, and D. P. Jackson, Phys. Rev. A **46**, 4894 (1992); D. P. Jackson, and R. E. Goldstein, and A. O. Cebers, Phys. Rev. E **50**, 298 (1994); J. A. Miranda, and M. Widom, Phys. Rev. E **55**, 3758 (1997); D. P. Jackson and B. Gantner, Phys. Rev. E **64**, 056230 (2001).
- <sup>8</sup> F. Elias, I. Drikis, A. Cebers, C. Flament, and J.-C. Bacri, Eur. Phys. J. B **3**, 203 (1998).
- <sup>9</sup> M. P. de Albuquerque and P. Molho, J. Magn. Magn. Mat. **113**, 132 (1992); *ibid.* **140**, 1869 (1995).
- <sup>10</sup> K. L. Babcock and R. M. Westervelt, Phys. Rev. Lett. **63**, 175 (1989); K. L. Babcock and R. M. Westervelt, Phys. Rev. A **40**, 2022 (1989).
- <sup>11</sup> C. Sagui and R. C. Desai, Phys. Rev. Lett. **71**, 3995 (1993); Phys. Rev. E **49**, 2225 (1994); Phys. Rev. E **52** 2807 (1995).
- <sup>12</sup> S. Courtin and S. Padovani, Europhys. Lett. **50**, 94 (2000); A. D. Stoycheva and S. J. Singer, Phys. Rev. E **65**, 036706 (2002); J. R. Iglesias, S. Goncalves, O. A. Nagel, and M. Kiwi, Phys. Rev. B **65**, 064447 (2002).
- <sup>13</sup> The present strategy can be seen to correspond to a ‘phase field’ approach. See L.-Q. Chen, Annu. Rev. Mater. Sci. **32**, 113 (2002).
- <sup>14</sup> P. M. Chaikin and T. C. Lubensky, *Principles of Condensed Matter Physics*, (Cambridge University Press, 1995).
- <sup>15</sup> C. Canuto, M. Y. Hussaini, A. Quarteroni, and T. A. Zang, *Spectral methods in fluid dynamics*, (Springer-Verlag, New York, 1988).
- <sup>16</sup> W. H. Press, S. A. Teukolsky, W. T. Vetterling, and B. P. Flannery, Numerical Recipes (Cambridge University, Cambridge, 1992).
- <sup>17</sup> C. B. Muratov, Phys. Rev. E **66**, 066108 (2002).
- <sup>18</sup> R. E. Goldstein, D. J. Muraki and D. M. Petrich, Phys. Rev. E **53**, 3933 (1996).
- <sup>19</sup> S. Miura, M. Mino, and H. Yamazaki, J. Phys. Soc. Japan **70**, 2821 (2001).
- <sup>20</sup> M. S. Pierce *et al.*, Phys. Rev. Lett. **90**, 175502 (2003); and private communication.
- <sup>21</sup> J. Swift and P.C. Hohenberg, Phys. Rev. A **15**, 319 (1977); H. Qian and G. F. Mazenko, Phys. Rev. E **67**, 036102 (2003); T. Galla and E. Moro, Phys. Rev. E **67**, 035101 (2003).